

**Princeton Plasma Physics Laboratory  
NSTX-U Experimental Proposal**

**Title: Rotation effects on Alfvén eigenmodes**

**OP-XP-1525**

Revision: **0**

Effective Date:  
*(Approval date unless otherwise stipulated)*  
Expiration Date:  
*(2 yrs. unless otherwise stipulated)*

**PROPOSAL APPROVALS**

**Responsible Author: Neal A. Crocker**

Date

**SG, TSG or TF Leader (assigned by RC):**

Date

**Run Coordinator (RC):**

**Jonathan Menard**

Date

**Responsible Division: Experimental Research Operations**

**RESTRICTIONS or MINOR MODIFICATIONS**

(Approved by Experimental Research Operations)

# NSTX-U EXPERIMENTAL PROPOSAL

TITLE: **Rotation effects on Alfvén eigenmodes**  
AUTHORS: **N. A. Crocker, M. Podestà,  
E. D. Fredrickson, N. N. Gorelenkov, E. Belova,  
H. Smith, K. Tritz, W. Guttenfelder, D. Gates**

No. **OP-XP-1525**  
DATE:

## 1. Overview of planned experiment

Toroidal rotation and rotation shear affect the structure and stability of several varieties of Alfvén eigenmodes in H-mode beam heated plasmas—in particular toroidicity-induced (TAE), compressional (CAE) and global (GAE) Alfvén eigenmodes. Varying rotation in a controlled way, e.g. through magnetic braking, may provide a means to affect mode stability and structure without directly affecting the fast ion population. The two main goals are (i) explore a potential control tool for the modes, and (ii) provide a set of data to challenge theories on AE stability and mode structure.

## 2. Theoretical/ empirical justification

Alfvén eigenmodes can have a significant impact on plasma performance. TAEs cause fast ion transport, while CAE and GAEs are thought to cause core energy transport. Toroidal rotation and rotation shear are expected to have a significant impact on the structure and stability of these modes.

TAEs and GAEs are shear Alfvén eigenmodes whose radial structures are strongly influenced by the radial structure of the Alfvén continuum. As shown in Fig. 1, rotation imposes a Doppler shift on the continuum (and the mode frequency) and rotation shear leads to a spatial variation of the Doppler shift, altering the structure of the continuum [M. Podestà et al., PoP 2010]. The structure of the continuum also plays a role in the stability of the modes, since it influences the interaction of the modes with the continuum, and the resulting continuum damping.

CAEs are compressional, approximately satisfying the dispersion relation  $\omega(\omega - n\omega_{ROT}) = k^2 V_{Alfvén}^2$ . Toroidal rotation shear imposes a spatial variation of the Doppler shift,  $n\omega_{ROT}$ , which affects  $k$  and the spatial structure of the mode.

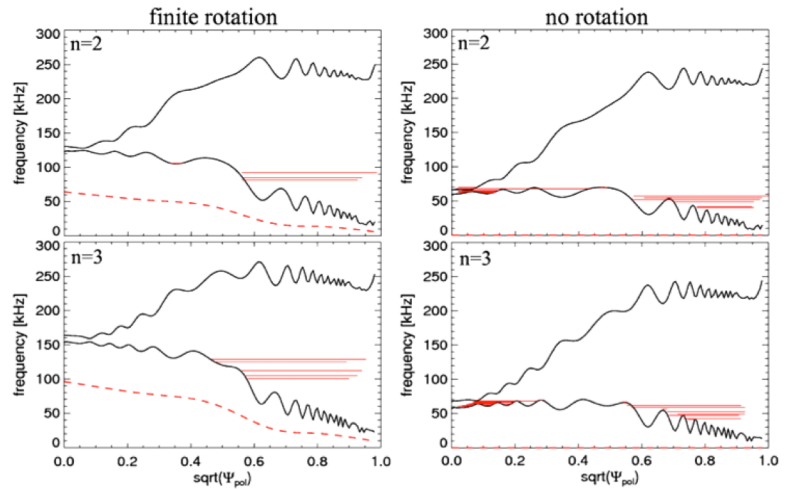


Fig. 1: Example of TAE gap for  $n=2,3$  modes from NOVA, computed with and without rotation. Dashed line is the frequency Doppler shift from rotation. Solid red lines indicate the location and frequency of TAE modes.

All three type of modes are excited by resonant interactions with fast ions, so the Doppler shift imposed by toroidal rotation also has an impact on their stability by shifting the resonances in phase space.

Experiments with braking in NSTX H-mode plasmas via an externally imposed  $n=3$  magnetic perturbation showed that it could be used effectively and reliably without causing severe degradation of plasma performance (e.g. without causing disruption).

### 3. Experimental run plan

The experiment requires an H-mode scenario susceptible to  $n=3$  braking that has high relative rotation in order to see a significant effect from the braking (i.e. high  $n f_{ROT}/f$  for modes with toroidal mode number and frequency  $n$  and  $f$ ). The modes are Alfvénic, so  $f \propto f_{\text{Alfvén}}$ , making higher density more desirable. However, mode structure measurements with the reflectometer array are necessary, so it is necessary to have monotonic density profiles with a maximum  $n_0 = 7 \times 10^{-13} \text{ cm}^{-3}$ . Prior to the experiment, a large range of plasma conditions will be surveyed, including in XP1520 “Ip/Bt scaling”, XP1523 “Characterization of 2nd NBI line” and in the list of baseline NTV braking capability shots. A suitable target plasma may be developed in this survey. However, in the absence of such data, experience from NSTX is used to develop the run plan.

In NSTX, TAEs tended to require high  $\beta_{fast}/\beta_{total}$  ( $> \sim 0.2$ ) for instability in NSTX, which tended to occur at low density,  $n_0 < \sim 4 \times 10^{-13}$ , for shots with modest beam power (4 MW). In contrast, CAEs and GAEs were more robustly unstable, so under similar conditions, the density would have been limited only by the requirement for mode structure measurements, to a maximum  $n_0 = 7 \times 10^{-13} \text{ cm}^{-3}$ . In light of these differences, the run plan includes provisions for optimizing and exploiting the first few hundred milliseconds of the current flattop, when density is low, for the study of TAEs. Since more parallel injection in NSTX-U may make TAEs more unstable, the maximum density for TAE instability may prove to be higher, alleviating this requirement.

Monotonic density profiles are required in order to facilitate mode structure measurements with the reflectometer array. This requirement may be easily fulfilled for the CAEs and GAEs. In NSTX, monotonic density profiles peaking at  $n_0 \sim 7 \times 10^{-13}$  were commonly achieved in H-mode discharges during the middle portion of the flattop. Unfortunately, it was uncommon to have monotonic profiles early in the flattop of H-mode discharges, when density was low enough for TAEs to be unstable, because edge impurity accumulation tended to make the profile hollow or flat until central density was high enough to stabilize TAEs. If low density proves to be a requirement for TAE instability, various measures will be attempted to flush the edge impurities during or at the end of the current ramp to make the density profile monotonic at the start of the current ramp. Such measures include deliberate dRsep jogs and/or ELM triggering with  $n=3$  RMPs. An important constraint for density reduction efforts is to avoid triggering low frequency MHD. The effect of low frequency MHD on the fast ion population would complicate efforts to compare the experimental results with theory for stability.

In NSTX, H-mode discharges typically exhibited a density ramp that would make reflectometer coverage spanning to the magnetic axis impossible during a significant portion of the discharge, in the latter part of the current flattop. Such coverage is highly desirable, so if initial operations point to a similar challenge in NSTX-U H-mode discharges, various measures may be attempted to slow the density ramp, such as

ELM pacing via  $n=3$  RMP pulses and dRsep jogs. Alternatively, it may be worthwhile to attempt to “reset” the density to a lower level at a strategic point in the flat-top by temporarily lowering beam power—possibly inducing a temporary L-mode period.

The run plan consists of 6 primary shots implementing different beam source mixes. There will be repeat shots as time permits, either revisiting interesting cases, or, if necessary using adjusted programming to address various contingencies.

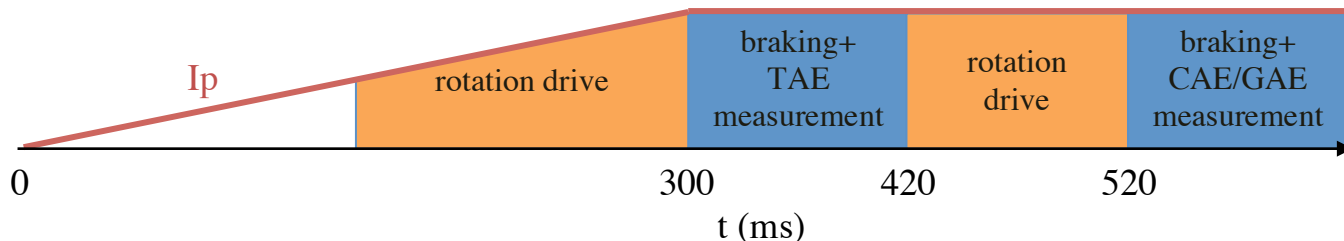


Figure 1: Illustration of sequence within shot.

Each of the primary shots will follow a similar pattern of two alternating periods of rotation drive and measurement (Fig. 1), with beam source mix variations during the measurement periods to change the spectrum of unstable modes. Braking with the  $n=3$  coils will be applied during the measurement periods to investigate the effects of rotation on mode structure and stability. The first rotation drive period will be during the current ramp, followed by a 120 ms measurement period optimized for studying TAEs at the beginning of the current flat-top. After another 100 ms drive period, there will be a second measurement period optimized for studying CAEs and GAEs. It is anticipated that the 2<sup>nd</sup> beam line will be more effective at driving rotation than the 1<sup>st</sup>, so it will be used during the drive periods. However, since it interferes with CHERS rotation measurements, it will be switched off and the 1<sup>st</sup> beam line will be used during the braking periods, except for occasional beam blips from the 2<sup>nd</sup> beam line.

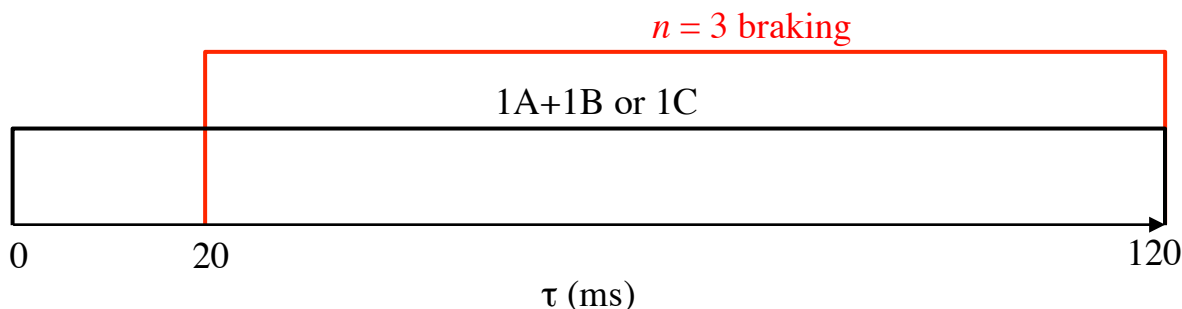


Figure 2: Braking and beam sequence within primary discharges 1 and 2

The first three primary discharges will have mixes consisting entirely of sources from beam line 1. For these discharges, an  $n=3$  braking pulse will be initiated 20 ms after the start of each measurement period to allow for mode structure and rotation measurements in the unbraked plasma. The first two of these discharges will combine 1A with 1B and 1C, respectively, during the measurement periods (Fig. 2). The third will combine 1B and 1C during the measurement periods, with 1B notches during the first and last 20 ms synchronized with 1A blips to allow MSE + CHERS measurements (Fig. 3). This timing allows for rotation and  $q$  profile measurements bracketing the measurement period to allow for interpolation of

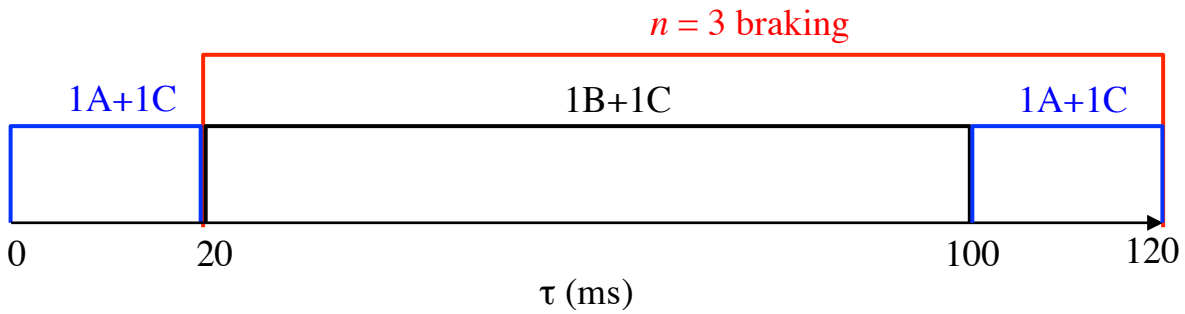


Figure 3: Braking and beam sequence within primary discharges 3

profiles within the period. The remaining three primary discharges will be similar to the third discharge, since the combination of 1B and 1C is expected to be minimally destabilizing to TAEs. However, they will include added blips from one of the 2<sup>nd</sup> beam line sources to investigate the instabilities excited by those sources (Fig. 4). There will be two blips from a 2<sup>nd</sup> beamline source lasting 20 ms starting at 20 ms and 80 ms, respectively, within the measurement period, and braking will be applied from  $t = 40$  ms to 120 within the measurement period. This time allows for mode structure and amplitude measurements of the excited modes by the first 2<sup>nd</sup> beamline blip in the unbraked plasma, and by the second 2<sup>nd</sup> beamline blip in the braked plasma.

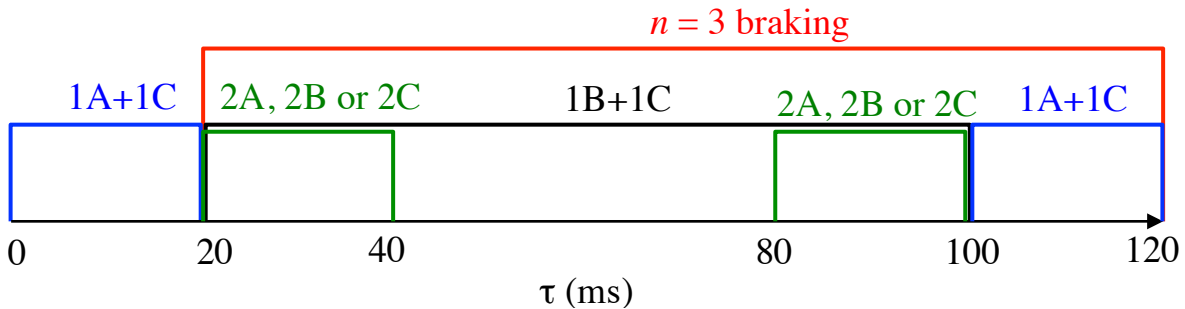


Figure 4: Braking and beam sequence within primary discharges 4 – 6

The sequence of beam source mixes is outlined below. The first three mixes are the highest priority, so the full run time may be used if necessary to achieve the three mixes with acceptable control of density and MHD. If all six mixes are completed, remaining time will be dedicated to repeat a “best-case” NB mix with scans of  $n=3$  braking amplitude.

Beam source mixes:

1. 1A (2 MW) + 1B (2 MW) (Fig. 2)
2. 1A (2 MW) + 1C (2 MW) (Fig. 2)

(2 MW of 1A blips synchronized with 1B notches in remaining discharge to allow MSE+CHERS measurements)

3. 1B (2 MW) + 1C (2 MW) (Fig. 3)
4. 1B (2 MW) + 1C (2 MW) + 2A (2MW) blips (Fig. 4)
5. 1B (2 MW) + 1C (2 MW) + 2B (2MW) blips (Fig. 4)
6. 1B (2 MW) + 1C (2 MW) + 2C (2MW) blips (Fig. 4)

## 4. Required machine, NBI, RF, CHI and diagnostic capabilities

The experiment needs 4MW of NBI to sustain well-reproducible beam heated H-mode plasmas. Various mixes of 1<sup>st</sup> and 2<sup>nd</sup> beamline sources are planned during measurement periods. 6 MWs from NBI2 will be required for rotation drive.

The experiment needs an established n=3 braking capability for H-mode plasmas in NSTX-U. This requirement may restrict the choices targets plasmas.

Toroidal rotation  $\Omega$  and density measurements and q profile are necessary, so 20 CHERS, MPTS and MSE are needed. This will place constraints on the use of NBI2 to facilitate CHERS measurements and  $\Omega$  requires source 1A for MSE.

Mode characteristics, including frequency structure and amplitude must be measured:

- It is necessary to have high frequency ( $f < \sim 2$  MHz) edge magnetic arrays for frequency and toroidal mode number measurements
- It is necessary to have the reflectometer array for radial mode structure; the 2010 Q- & V-band capability penetrate to equilibrium density of  $7 \times 10^{13} \text{ cm}^{-3}$ .
- It is desirable to have BES outer core/edge 2D structure measurements.

It may be necessary to use lithium conditioning. Monotonic density profiles are necessary for the reflectometer array measurements.

It is necessary to have target plasmas with high relative rotation speed,  $f_{\text{ROT0}}/f_{\text{Alfvén0}}$ , to allow for a significant effect from braking for CAEs and GAEs. It may be necessary to operate at low BT (e.g. BT = 0.45T) to get high rotation while simultaneously making core reflectometer measurements.  $f_{\text{ROT0}}/f_{\text{Alfvén0}} > 0.2$  was achievable in NSTX H-Mode at  $P_{\text{NBI1}}=6$  MW, BT = 0.45 &  $n_0 = 7 \times 10^{13} \text{ cm}^{-3}$  (shot 141398, t = 580 ms). Under those conditions  $f_{\text{Alfvén0}} \sim 90$  kHz,  $f_{\text{ROT0}} \sim 20$  kHz. Pre-spinning the plasma to high velocity with NBI2 may allow for higher BT and/or lower  $n_0$ .

TAEs are more sensitive to rotation: it is necessary to have high  $f_{\text{ROT0}}/f_{\text{TAE0}} = 2q_0 f_{\text{ROT0}}/f_{\text{Alfvén0}}$ . So, higher BT may be acceptable.

It may be necessary to have low density ( $n_0 < \sim 4 \times 10^{13}$ ) during the first 120 ms of the current flattop. In NSTX high  $\beta_{\text{fast}}/\beta_{\text{total}}$  ( $> \sim 0.2$ ) was needed for TAE instability.

Monitoring of the fast-ion population as rotation is changed is highly desirable, so FIDA and ssNPA arrays are highly desirable. Also, other fast ion population diagnostics are desirable.

## 5. Planned analysis

The primary analysis will be to compare the composition of observed spectrum and the measured structure and frequency of the modes with appropriate codes: NOVA-K for TAEs, HYM for GAEs, HYM + CAE3B (H. Smith) + CAE (E. Fredrickson) for CAEs. (NOVA-K and HYM predict growth rates; CAE3B and CAE only give structure and frequency.) A possible secondary analysis will be to assess the affects of the modes on core energy and fast-ion transport as a function of rotation. The feasibility of

transport analysis will depend on the ability to account for redistribution of fast-ions from other causes such as low frequency MHD.

## 6. Planned publication of results

The results will be presented at IAEA and APS meeting and published in appropriate journals such Nucl. Fusion, PPCF and Physics of Plasmas.

## 7. Estimated Neutron Production

Based on the number of shots, plasma current levels, and expected durations, estimate the maximum neutron production of this experiment. See calculator in Appendix #2 for this calculation.

# of Shots used in Estimate: \_\_\_\_\_ Estimated Total Neutron Production: \_\_\_\_\_

# PHYSICS OPERATIONS REQUEST

TITLE:  
AUTHORS:

No. **OP-XP-**  
DATE:

*(use additional sheets and attach waveform diagrams if necessary)*

**Brief description of the most important operational plasma conditions required and any special hardware requirement:**

- (1) 4 MW NBI H-mode (various mixes of 1<sup>st</sup> and 2<sup>nd</sup> beamlines with sources at 2 MW)
- (2) High rotation (e.g.  $f_{\text{ROT0}}/f_{\text{Alfvén0}} > 0.2$  if possible), which may require low  $B_T$  (e.g.  $B_T = 0.45$  T)
- (3) Substantial  $n = 3$  braking (e.g.  $\Delta f_{\text{ROT0}}/f_{\text{ROT0}} \sim 1/2$  if possible)
- (4)  $n_0 < \sim 4 \times 10^{-13}$  during 1<sup>st</sup> 120 ms of current flattop for TAE instability
- (5)  $n_0 < \sim 7 \times 10^{-13}$  and monotonic  $n(r)$  until  $t = 640$  ms for reflectometer measurements
- (6) Monitoring of fast-ion population

**Previous shot(s) which can be repeated: TBD**

**Previous shot(s) which can be modified: TBD**

**Machine conditions** (*specify ranges as appropriate, strike out inapplicable cases*)

$B_T$  Range (T): < 0.65                      Flattop Duration (s): 340 ms

$I_p$  Range (MA):                                      Flattop Duration (s): 340 ms

Configuration: **LSN**

Equilibrium Control: ??? **Outer gap / Isoflux (rtEFIT) / Strike-point control (rtEFIT)**

Outer gap (m):                                      Inner gap (m):                                      Z position (m):

Elongation:    Triangularity (U/L):                                      OSP radius (m):

Gas Species:    Injector(s):

**NBI Species: D**                                      Heating Duration (s):  $\sim 500$  ms

Voltage (kV)    50 cm (1C):    90            60 cm (1B):    90            70 cm (1A):    90

Voltage (kV)    110 cm (2C):    90            120 cm (2B):    90            130 cm (2A):    90

**ICRF Power (MW):** N/A            Phase between straps (°):                      Duration (s):

**CHI:** N/A                                      Bank capacitance (mF):



**LITERS: On** Total deposition rate (mg/min) or dose per discharge (mg): ???

**EFC coils: On**

## DIAGNOSTIC CHECKLIST [1]

TITLE:  
AUTHORS:

No. **OP-XP-**  
DATE:

*Note special diagnostic requirements in Sec. 4*

Diagnostic	Need	Want
Beam Emission Spectroscopy		x
Bolometer – midplane array		
CHERS – poloidal		x
CHERS – toroidal	x	
Divertor Bolometer (LADA)		
Divertor visible cameras		
Dust detector		
Edge deposition monitors [2]		
Edge neutral density diag.		
Edge MIGs [2]		
Penning Gauges [2]		
Edge rotation diagnostic		x
Fast cameras – divertor [2]		
Fast ion D <sub>α</sub> - poloidal	x	
Fast ion D <sub>α</sub> - toroidal	x	
Fast lost ion probes - IFLIP		x
Fast lost ion probes - SFLIP		x
Filterscopes [2]		
FIReTIP		x
Gas puff imaging – divertor		
Gas puff imaging – midplane		
H $\alpha$ cameras - 1D [2]		
Infrared cameras [2]		
Langmuir probes – divertor		
Langmuir probes – RF		
Langmuir probes – RF ant.		
Magnetics – Diamagnetism		
Magnetics – Halo currents		
Magnetics – RWM sensors		

*Note special diagnostic requirements in Sec. 4*

Diagnostic	Need	Want
MAPP		
Mirnov coils – high f.	x	
Mirnov coils – toroidal array	x	
MSE-CIF	x	
MSE-LIF		x!
Neutron detectors [2]	x	
Plasma TV		
Reflectometer – 65GHz		
Reflectometer – correlation		
Reflectometer – FM/CW		
Reflectometer – fixed f	x	
Reflectometer – SOL		
SSNPA [2]	x	
RF edge probes		
Spectrometer – divertor		
Spectrometer – MonaLisa		
Spectrometer – VIPS		
Spectrometer – LOWEUS		
Spectrometer – XEUS		
TAE Antenna		
Thomson scattering	x	
USXR – pol. Arrays		
USXR – multi-energy		
USXR – TG spectr.		
Visible Brems. det. [2]		

Notes:

[1] Check marks in this table do not guarantee diagnostic availability. Check with diagnostic physicists or research operations management to ensure diagnostic coverage.

[2] In some cases, a given line represents multiple diagnostics. For instance, there are multiple SSNPAs, multiple IR cameras, multiple neutron detectors, and multiple Langmuir probe arrays.

## Appendix #1: Allowed Neutral Beam Power vs. Pulse Duration

Heating of the primary energy ion dump limits the beam duration to that given in the following table<sup>1</sup>:

Acceleration Voltage [kV]	MW per Source	MW per Beamline	Pulse Length [s]
65	1.1	3.2	8
70	1.3	3.8	7
75	1.5	4.5	6
80	1.7	5.1	5
85	1.9	5.8	4
90	2.1	6.4	3
95	2.4	7.1	2
100	2.6	7.7	1.5
105	2.8	8.4	1.25
110	3.0	9.0	1

Table A1: Beam power and pulse length as a function of acceleration voltage

## Appendix #2: Table for neutron rate estimations:

Change only the blue cells					
$I_p$ Range [kA]	Center of $I_p$ Range [kA]	Number of Discharges	Typical Discharge Time [s]	Assumed Neutron Rate [N/s]	Fluence at this $I_p$ [N]
$0 < I_p \leq 400$	200	0	0	0.00E+00	0.00E+00
$400 < I_p \leq 600$	500	0	0	1.00E+14	0.00E+00
$600 < I_p \leq 800$	700	0	0	2.00E+14	0.00E+00
$800 < I_p \leq 1000$	900	1	1.5	3.00E+14	4.50E+14
$1000 < I_p \leq 1200$	1100	10	1	4.00E+14	4.00E+15
$1200 < I_p \leq 1400$	1300	0	0	5.00E+14	0.00E+00
$1400 < I_p \leq 1600$	1500	15	4	8.00E+14	4.80E+16
$1600 < I_p \leq 1800$	1700	1	1	1.30E+15	1.30E+15
$1800 < I_p \leq 2000$	1900	0	0	2.00E+15	0.00E+00
Total # of Discharges		27	Total Fluence		5.38E+16

Table A2: Neutron Emission Rate Calculator. Double click to open in excel for automatic calculation. Change only the blue cells.

<sup>1</sup> J.E. Menard, et al., Nuclear Fusion **52**, 2012 (83015)